Design of FRC tunnel segments considering the ductility requirements of the Model Code 2010

Liao Lin, Albert de la Fuente, Sergio Cavalaro, Antonio Aguado

Polytechnic University of Catalonia (UPC) BarcelonaTech, Barcelona, Spain.

* Corresponding author. Tel.: +34-93-401-65-15. e-mail: albert.de.la.fuente@upc.edu

Abstract

Fibre reinforced concrete (FRC) is used to improve the mechanical response of precast segments for tunnels. The structural use of the material has been regulated by national codes and, recently, by the Model Code 2010 (MC 2010, hereinafter). In this regard, it is necessary to update the philosophy applied to the design of tunnel segments in compliance with the most recent guidelines, evaluating their applicability and repercussion. The objective of this paper is to present a critical analysis of the design of FRC segments according to the ductility requirements from the MC 2010; an alternative approach is proposed that is compatible with the condition found in some tunnels. The repercussions of both approaches are evaluated for the Metro Line 9 from Barcelona using results obtained in an experimental program with full-scale segments. The study suggests that the alternative approach may be applied under certain conditions, leading to a reduction in the fibre consumption.

Keywords*: Barcelona Metro Line, Cracking bending moment, design, ductility, FRC, precast segments.*

1 INTRODUCTION

Fibre reinforced concrete (FRC) is a composite material used to improve the mechanical response of precast segments for tunnels [1-4], enhancing their ductility and fire resistance as well as their mechanical performance during transient load stages. Due to these advantages, the use of structural fibres contributes to the replacement of traditional passive reinforcement, accelerating the production process and increasing the competitiveness of the FRC. Proof of this are the numerous experiences in which precast FRC segments have been used in highway (RT), railway (RWT), metro (MT), water supply (WTT), gas transport (GPT) and service (ST) tunnels. Table 1 [4-6] summarizes some of the main applications already in service or under construction.

The structural use of fibres has been regulated by the national codes in Germany in 1992 [7], Italy in 2006 [8] and Spain in 2008 [9], for instance. More recently, recommendations about the design of FRC structures were also included in the MC 2010 [10], with constitutive equations [11-12] and models for the Service Limit State and Ultimate Limit State (SLS and the ULS, respectively). An increase in the use of FRC in tunnels segments has been observed as a result of that [13]. In this regard, it is necessary to update the philosophy applied to the design of tunnel segments in compliance with the particular requirements proposed in the MC 2010, evaluating its applicability and repercussions.

The objective of this paper is to present a critical analysis of the design of FRC segments according to the ductility requirements from the MC 2010 and to propose an alternative approach more compatible with the conditions found in practice. First, the design procedure from the MC 2010 is analysed and adapted to FRC segmented linings. Then, the alternative approach is presented. The applicability and repercussion of both approaches in terms of fibre consumption are evaluated in the specific case of the Metro Line 9 from Barcelona, using sectional analysis and results obtained in an experimental program with real-scale segments. This study shows the possible consequences of applying the design philosophy of the MC 2010 for FRC segments and it indicates alternative design considerations that could be implemented if certain conditions are fulfilled and it provides an example on how it may be used to optimize the fibre content required.

2 DESIGN PROCEDURE BASED ON THE MC 2010

In tunnels with large internal diameter, segments are usually subjected to high bending moments during the transient and the service stages - the latter being generally the most unfavourable design condition. The replacement of traditional reinforcement by fibres is limited, generally leading to expensive solutions since high amounts of fibre are needed to achieve an equivalent mechanical response. In these cases, mixed reinforcement configurations consisting of a minimum amount of steel bars (that provide resistant capacity in ULS) and a moderate dosage of fibres (that control the crack width in SLS) are attractive solutions.

On the other hand, tunnels with smaller internal diameter tend to be predominantly compressed during service, these being less sensible to either asymmetric loads derived from the soil or other discontinuities. As a result, the main reinforcement usually consists of a minimum amount of

rebars established in codes to avoid brittle failure of the segments that might occur during the transient load situations. In such cases, the complete substitution of the traditional reinforcement by fibres may be a suitable alternative from the technical and the economic points of view.

The most relevant transient situations correspond to the demoulding, stocking, transport, manipulation, and the placement of the segments inside the tunnel and the application of the thrust forces by the jacks [13-17], as shown in Figure 1. The SLS and ULS limit conditions considered in the structural verification in each one of these transient situations vary depending on the load pattern applied. For instance, the demoulding, the stocking, the transport and the manipulation are characterized by load patterns that induce bending moments and might generate bending cracks or failure. Conversely, the placement of the segments, and the application of the thrust forces are characterized by a concentrated load in a reduced area that might generate localized cracking.

Although verifications should be performed for both types of load patterns, the first is directly related with the design guidelines provided by the MC 2010 for FRC, whereas the bursting and the splitting require special considerations [18-22]. Therefore, considering the main objective of the paper, only the transient load situations that lead to bending are analysed here.

If fibres are applied as the only reinforcement, the MC 2010 imposes three mechanical criteria based on the load – displacement curve shown in Figure 2a that any FRC structure should fulfil. First, the ultimate load (P_u) resisted shall be higher than both the cracking (P_{cr}) and the service (P_{SLS}) loads. Second, the ultimate vertical displacement (δ_u) should be larger than the observed in the service limit state (δ_{SLS}) calculated performing a linear elastic analysis with the assumptions of uncracked concrete and initial elastic Young's modulus. Third, the δ_{SLS} should be at least 5 times lower than the vertical displacement δ_{peak} estimated for the maximum load (P_{max}).

The first requirement about the ultimate load is a condition established in most reinforced concrete codes that intend to avoid the brittle failure in case of cracking ($P_u \geq P_{cr}$). This requirement may be translated in terms of the bending moment through the equivalent relation $M_u \geq M_{cr}$ [5-6; 23-25], in which M_u and M_{cr} are the ultimate and the cracking bending moments, respectively. The restriction $P_u \geq P_{SLS}$ ($M_u \geq M_{SLS}$) is rarely limiting the design of precast segments for tunnels since bending moments are usually small and $P_{cr} \geq P_{SLS}$ ($M_{cr} > M_{SLS}$) during transient situations. In this sense, cracking is rather caused by accidental loads or even to inadequate support or handling of the segment and should be treated differently [26-28]. Hence, the condition $M_u \geq M_{cr}$ tend to be the most restrictive condition regarding the ultimate load.

The two displacement requirements ($\delta_u \geq \delta_{SLS}$; $\delta_{peak} \geq 5\delta_{SLS}$) intend to guarantee a minimum deformability of the most unfavourable sections in order to activate the redistribution capacity of statically indeterminate structures. It is important to remark that precast segments tend to assume a statically determinate configuration during the transient stages. Therefore, in this case the deformability requirements would not be necessary since the condition $M_u \geq M_{cr}$ is sufficient to guarantee the ductility in case of a hypothetical flexural rupture [4-6; 23-25]. Consequently, the minimum reinforcement according with the MC 2010 is determined by the ductility requirement expressed through $M_u \geq M_{cr}$.

The moment-curvature diagram ($M - \chi$) presented in Figure 2b includes different reinforcement configurations (infracritical, critical and supracritical) [23]. Notice that by imposing M_u

$\geq M_{cr}$, only critical and supracritical reinforcement configurations are allowed according to the design philosophy from the MC 2010. Needless to say that if the design bending moment M_d is higher than M_{cr}, the requirement to be imposed shall be $M_u \geq M_d$ [29-32]. This means that a supracritical reinforcement arrangement should be used (Fig. 2b), thus making the total replacement of the rebars by fibres less competitive.

To determine the minimum amount of fibre reinforcement required, the condition $M_u \geq M_{cr}$ must be solved by using nonlinear sectional analysis (Fig. 3) and by imposing the constitutive equations suggested in the MC 2010. In this sense, a rigid-plastic response may be assumed to simulate both the compressive and post-cracking tensile responses of the FRC. By doing so, the residual flexural tensile strength related to a crack mouth opening displacement of 2.5 mm (f_{R3}) can be derived and established as a control parameter for the tests to be performed during production. This criteria related to the deformation is also adopted in the MC 2010 as a reference for the verification of the ULS of FRC structures.

In typical transient load situations observed in practice, a simple bending condition may be expected. Equations (1) and (2) are derived by imposing the equilibrium conditions and by assuming external axial forces are $N \approx 0$ (these forces are usually small and their exclusion leads to results on the safe side as they tend to produce compressed in the cross – sections).

$$N = f_c b \lambda x_n - f_{Ftu} b (h - x_n) = 0 \tag{1}$$

$$N = f_c b \lambda x_n \frac{5h - x_n}{10} = M_u \tag{2}$$

In Equations 1 and 2, f_c is the uniaxial compressive strength of the concrete, f_{Ftu} is the residual tensile strength of the FRC, b is the width of the segment, h is the height of the segment, and x_n is neutral axis depth. The value adopted here for the parameter λ is 0.8 (4/5), according to the recommendation of the MC 2010.

Equations (1) and (2) may be combined to obtain Equation (3) that provides the required value of f_{R3}. It should be emphasized that depending on the limit state analysed, the partial safety factors for both the material and loads might differ. Moreover, the time dependency of f_{R3} and f_c should be taken into account as well.

$$f_{R3} \geq \frac{12 f_c}{\frac{1}{\left(-1+\sqrt{1+2\frac{M}{f_c b h^2}}\right)} - 5} \tag{3}$$

According to the MC 2010, the minimum average value of f_{R3} ($f_{R3m,min}$) is derived imposing in Equation (3) the condition $M_u = M_{cr} = b \cdot h^2 \cdot f_{ctm,fl}/6$, with the average compressive strength (f_{cm}) and the average flexural tensile strength ($f_{ctm,fl}$) of concrete. As a result, Equation (4) is obtained. Notice that the calculation is performed with average values of loads and material properties. Moreover, the $f_{R3m,min}$ required depends solely on the mechanical properties of concrete. Thus, should the mechanical properties of the material increase with time, $f_{R3m,min}$ would also increase.

$$f_{R3m,min} = \frac{12 f_{cm}}{\frac{1}{\left(-1+\sqrt{1+\frac{f_{ctm,fl}}{3 f_{cm}}}\right)}} - 5 \quad (4)$$

As an example of application, the curves $f_{R3m,min}$ versus time calculated for concrete strength classes C30, C50 and C70 are shown in Figures 4a, 4b and 4c, respectively. Furthermore, these curves are particularized for a representative range of h; 0.2 – 0.5 m being representative heights for precast concrete segments. The time dependency of the mechanical parameters involved in the formulation was considered by means of the expressions suggested in the MC 2010. Figure 4d summarizes the influence of the thickness h on $f_{R3m,min}$ for the same concrete classes.

The results presented in Figure. 4 highlight that the $f_{R3m,min}$ required decreases as h increases. Moreover, it is observed that $f_{R3m,min}$ increases with time due to the time dependency of $f_{ctm,fl}$ and of f_{cm}. Such an observation might lead to the erroneous conclusion that higher fibre contents would be required if the segment is subjected to the transient loads at later ages. Nevertheless, it is important to consider that, for the same fibre content, the f_{R3} also increases with the concrete age. Therefore, even though the value of $f_{R3m,min}$ required increases with time, the fibre content C_f probably will not increase since the pull – out mechanism also improves with time.

Despite that, apparent contradictions may arise from the data in Figure 4. Suppose the hypothetical case of a segment designed to be transported 7 days after of production that had its transport delayed by additional 7 days. The magnitude and the variability of the transient loads are often well established during the project phase (far better than the soil loads, for instance) due to the systematic and controlled production processes [**33**]. In fact, these actions should not vary considerably unless changes in the production process are introduced. Hence, the cracking safety factor should increase with time since $f_{ctm,fl}$ also increases. In other words, even though it would be safer to transport the segment at later ages, a higher $f_{R3m,min}$ would be required according to the results presented in Figure 4. A similar situation would be observed, for example, if the concrete used present a higher compressive strength than the originally defined in the project. In this case, a higher $f_{ctm,fl}$ would be obtained and higher values of $f_{R3m,min}$ are necessary to guarantee a ductile response of the segment despite having in reality a higher cracking safety factor.

The paradox would be even more evident if this philosophy was applied for a tunnel in which the thickness of the segment is governed by limitations of the TBM jacks (minimum height of the segment to fit the jack, for instance). In this case, $M_{cr} \geq M_d$ and, consequently, when the ductility limitation is applied, the $f_{R3m,min}$ derived from this requirement would correspond to a load that is higher that used for the ULS, whose probability of being surpassed is not relevant. In this context, one might question if it is reasonable to provide ductility for a load that is higher than that considered in the ULS for a transient stage.

This issue concerns the considerations included in the new design philosophy of the MC-2010 when applied to segmented linings. It is evident that for safety reasons a minimum ductility must be maintained to avoid brittle failure. The main issue is how such ductility should be defined in the case of segmented linings. To provide a reasonable alternative, it is important to consider the special context in which these elements are designed and used.

As mentioned before, in certain tunnels, segments are designed not to crack in transient stages and in service, presenting enough safety margins to account for the safety coefficients proposed in codes. For this reason, the likelihood of cracking is already contemplated in the design of the segments. Moreover, in tunnels subjected to mainly compressive loads in service (except in particular stretches), the transient load cases tend to be the critical ones. These are observed for a short period, before the elements have to fulfil their service life under controlled conditions. Consequently, if cracking due to imperfections or other damages occur, they may be detected and corrected before construction of the tunnels with small or even no repercussion to the performance of the structure and to the safety of workers. Another relevant aspect is that, in transient stages, the segments are normally subjected to statically determinate support configurations [29-32]. Therefore, no stress redistribution should be expected, thus reducing the justification for a critical or supercritical ductility.

In this context, the use of a residual strength that leads to a critical or supercritical ductility does not seem compatible with the stress produced due to the transient loads. If segments are designed not to crack, this criterion is excessively severe and could provide a structural response above the required for safety reasons, resulting in an overestimation of the minimum residual strength needed. To avoid overestimations, an alternative definition of the minimum ductility is proposed in the present study for the segmented lining.

Notice that the load applied in transient stages is mainly the result of the self-weight of the segments, which does not vary excessively due to the quality control of the precast producer. If by any chance cracking occurs, it should be the result of thermo-hygrometric stresses (induced, for instance, by shrinkage) or due to impacts that are limited in time. In both cases, the load that generates the crack tends to dissipate in a short time; as soon as the cracks are formed the stresses are released. To provoke the failure in such situation, the remaining load or that applied in later stages must be high enough to increase the crack opening. Taking into consideration that thermo-hygrometric induced stresses or impacts dissipate soon after the crack is formed, the only remaining load that could increase the crack opening up to failure would be expected during the posterior transient stages. As long as the remaining resistant capacity of the cracked cross – section is enough to resist theses loads, in addition to a safety margin introduced by the partial safety factor of the material and the load, the ductile failure would be assured.

Therefore, instead of estimating the minimum residual strength from the average cracking bending moment, a load-based criterion is suggested to assure ductility compatible with the load actually applied in the transient stages. This strength is calculated with the design values of the forces that act on the segment taking into account the corresponding safety factors for the materials and the actions (those suggested in the MC 2010, for instance). Such load-based criterion could yield the structural response indicated in the dotted curve from Figure 2b. This way, if cracking occurs for the reasons mentioned previously, the segment would still present enough ductility to safely carry the loads applied. It is important to remark that the alternative approach proposed here should be applied only if the segments are designed not to crack, the tunnel is subjected mainly to compression in the service stage and the critical load occurs in the transient stages under controlled conditions.

Taking the example of an element subjected to a bending moment (included in this section), the required $f_{R3m,min}$ according to the alternative approach proposed ($f_{R3m,alt}$) may be obtained through Equation (5). This equation includes the concrete safety factor (γ_c) that is multiplied by the design strength f_{R3} required (f_{R3d}) to obtain the characteristic value of f_{R3} (f_{R3k}). The letter is divided by the coefficient ψ, intended to transform characteristic values of the tensile strength in average values. The f_{R3d} may be substituted by Equation (3) if the design compressive strength (f_{cd}) and the design bending moment (M_d) calculated with the partial safety factors are used.

$$f_{R3m,alt} \geq \frac{\gamma_c}{\psi} f_{R3d} = \frac{\gamma_c}{\psi} \frac{12 f_{cd}}{\frac{1}{\left(-1+\sqrt{1+2\frac{M_d}{f_{cd} b h^2}}\right)} - 5} \quad (5)$$

Equation (5) implies that the service loads do not affect the minimum f_{R3} value estimated, regardless of the nature of the load applied. For example, in case of a tunnel subjected to asymmetric seismic loads, the alternative approach should be valid as long as the design loads are not high enough to produce cracks in the segments and the transient stages still represent the critical condition. Otherwise, a specific analysis should be performed.

To evaluate the repercussion of the ductility criteria proposed here and defined by MC 2010 in terms of fibre consumption, their application to the Metro L9 of Barcelona is presented in the next section.

3 METRO L9 OF BARCELONA

The Metro L9 of Barcelona counts 46 stations and 15 interchanges with a total length of 44 km and connects the airport (El Prat), the justice district (Ciutat de la Justicia) and the high speed railway station (Barcelona Sants Station). The construction is performed with a TBM with approximately 12.0 m of diameter. So far, this is probably one of the most studied TBM-bored tunnels and this is still under construction. In this sense, experimental and numerical analysis related with the FRC were extensively performed [34-37]. Likewise, particular numerical studies concerning the concentrated load induced by the jacks were also developed to explain some of the cracks observed during the construction of the tunnel [38].

The Bon Pastor – Can Zam stretch is analysed in the present study. It consists of a ring with D_i = 10.90 m and this is divided in 7 segments and 1 key with h = 0.35 mm and b = 1.8 mm. The segments were initially designed with a C50/60 concrete reinforced with traditional rebars and 30 kg/m^3 of steel fibres. The structural contribution of the fibres was originally not considered in the design. These were only intended to reduce the incidence of damages due to impact during manipulation and placing of the segments. Figure 5 shows the layout of the ring and the reinforcement used.

3.1 Numerical simulations

In this context, the total substitution of the rebars by steel fibres was analysed. First, a numerical study considering the possible load cases was developed in order to verify the suitability of

this reinforcement strategy. The results of this analysis were reported in [34]. The main conclusions derived were the following:

- The worst load condition is expected during the stocking. After demoulding, only three segments can be stacked to avoid concrete cracking. The remaining segments of the ring can be stacked seven days after casting. This load situation was analysed in detail since this is critical in terms of design and productivity.

- The advance of the TBM during construction is accomplished by means of 15 jacks that have a contact area of 1.374 x 0.350 m^2 and introduce a total force of 90 MN in the segmented lining. This load situation was simulated considering 35 mm of eccentricity of the thrust jacks (see Figure 6). The numerical results indicated the presence of bursting stresses in the disturbed zone generated by this local force. The tensile stresses reach values above the tensile strength of concrete (f_{ct}). Therefore, cracking of the concrete is highly probable during the construction of the tunnel due to the application of the thrust loads of the jacks. Fortunately, fibres contribute, bridging cracks and controlling their width. Besides, this is a transient load phase, and once the tunnel is in service, the cracks tend to close due to the compression introduced by the soil.

- The behaviour of the supports and their interaction with both the soil and water was also analysed numerically. Fourteen load cases were studied considering the existence of plastic hinges in the radial joints. The tensile stresses obtained with the model were below 0.785 N/mm^2 for the worst – case scenario, meaning that the cross – section of the segments conserve its integrity during the service life unless cracks appear during the stocking or other transient load situations. In any case, this stress level is low and the concrete cracking due to bending combined with axial loading is unlikely to occur. Therefore, it was concluded that the ring is subjected to compression during its service life and the reinforcement is mainly needed to control the crack widths during the transient load situations.

3.2 Experimental programs

3.2.1 Materials

Once identified with numerical analysis that the critical load occurs in the transient stage during stocking, an experimental program was conducted with real-scale segments in order to verify the substitution of the steel rebars by fibres. The composition of the concrete is presented in Table 2. Mixes were produced with different steel fibre contents (C_f) of 20, 30, 40, 50 and 60 kg/m^3 in order to assess the mechanical performance of the FRC with different amounts of fibres [34]. With this regard, hooked-end steel fibres with a length (l_f) of 50 mm, a cross – section diameter (d_f) of 1.00 mm and a yielding strength (f_f) of 1100 N/mm^2 were used. The amount of superplasticizer added to the concrete increased with the fibre content to assure similar workability (4 cm of slump in the cone test) and equivalent behaviour in terms of fibre distribution inside the segment [39-41], which is essential for the comparison of the structural responses.

From each composition, four prismatic specimens with 150x150x600 mm^3 were cast and cured under conditions that emulate those experienced of the segments. They were cured during 6

hours at 40 ºC and 80% of relative humidity. After that, they were stored at 20 ºC and 50% of relative humidity during 7 days. Finally, they were kept under the conditions of the production hall and tested at 28 days according with the standard UNE-EN 14651 [42] to characterize the limit of proportionality f_{LOP} and the residual flexural strengths f_{R1} and f_{R3}. The average values of f_{LOP}, f_{R1} and f_{R3} (f_{LOPm}, f_{R1m} and f_{R3m}, respectively) are included in Figure 7, along with the corresponding coefficient of variation.

The results summarized in Figure 7 highlight that the mechanical properties measured tend to increase with C_f, which is consistent with the results from [43]. It is important to remark that the FRC showed a softening behaviour in all cases. A linear regression of the data included in Figure 7 leads to Equations (6) and (7) for the assessment of the f_{R1m} and f_{R3m} depending on C_f (in kg/m^3). In the present study, these equations are considered as a reference to estimate the C_f needed in the design of the segments.

$$f_{R1m} = 0.063C_f + 1.64 \quad (6)$$

$$f_{R3m} = 0.089C_f \quad (7)$$

3.2.2 *Real scale tests related with the stocking procedure*

The numerical approach proposed to estimate f_{R3} was compared with the results derived from the experimental program on full-scale tests reproducing the stacking process. Even though FRC with a wide range of fibre contents were tested to evaluate the repercussion of the ductility criteria proposed by the MC 2010 in terms of design, segments reinforced with traditional rebars and 30 kg/m^3 of fibre and segments reinforced with 60 kg/m³ of fibres were produced for real-scale tests.

During the storage (Figure 8), the supports placed at the bottom of the pile are fixed, whereas the supports placed between adjacent segments should be aligned vertically without inducing eccentricities. In practice, however, slight deviations from the perfect alignment may occur in the support between segments. This generates bending moments and, ultimately, damages if M_{cr} is exceeded. Although the first segment from the pile has the highest loading, the critical load case in terms of bending moment is likely to occur in the second segment since it may be subjected to a larger eccentricity.

Tests were performed to evaluate the performance of segments if eccentricities are present. For that, they were stored in piles. The first segment was placed over the fixed support. Then, the second segment was positioned over the supports that had an eccentricity equal to e_e with the axis of the fixed support at the base of the pile. Next, the third segment was placed with an eccentricity e_i with respect to the axis of the fixed support at the base (Figure 8). Since a symmetric configuration is assumed to generate the highest bending moment, the theoretical free span that should exist in an ideal situation (l_o=2.8 m) for the second segment was increased by a distance of $2e_e$. Moreover, the total eccentricity e_{tot} applied for the third segment to the second one at each loading point was equal to e_e + e_i. Finally, the other segments that compose a ring were placed over the existing pile, achieving the configuration of 8 segments (7 + the key segment) depicted in Figure 8.

During the stacking process, the number and the width of cracks were measured. For that, two transducers were placed at both sides of the second segment (see Figure 8), close to the bottom of the lateral face that form the circumferential joint (indicated by T1). An additional transducer was

installed along the imaginary line that connects the support and the point of application of load to capture possible shear strains (indicated by T2)

The accidental values for e_e and e_i expected during construction are close to 0.10 m [34]. Since the aim of the experimental program was to evaluate the mechanical response of the segments with two different reinforcement strategies, values of $e_e = e_i = e$ were set to 0.25 m and to 0.50 m. Notice that the latter represents an exaggeration intended to force that $M_d > M_{cr}$, in order to favour concrete cracking and the activation of the reinforcement.

Figure 9a presents the results obtained in terms of total crack width (average value measured by the transducers T1 placed at both lateral faces) versus the number of segments in the pile (n_s). It is evident that the segment with mixed reinforcement (rebars + 30 kg/m^3 of fibres) shows a ductile behaviour. The crack occurred when the 6th segment was placed (4 segments stacked over the 2nd segment). Nevertheless, additional segments could be staked since the bars and the fibres became active after cracking, hence limiting the total crack opening to a value of 0.4 mm. In this sense, a variation of curve may be observed for values of n_s between 5 and 6, confirming a change of stiffness due to cracking.

The segment with 60 kg/m^3 of fibres and an eccentricity e of 0.50 m also cracked when the 6th segment was placed. The results highlight that the amount of 60 kg/m^3 of fibres was insufficient to guarantee a ductile behaviour in this case since a wide crack appeared and a brittle failure took place (Fig. 9b). On the other hand, the results indicate that the segment with 60 kg/m^3 of fibres and eccentricity e of 0.25 m presents a linear elastic behaviour during the complete test, showing no visible crack. In the next section, this phenomenon is studied through a numerical analysis.

4 ANALYSIS OF SECTIONAL RESPONSE

The structural analysis based on the design approaches presented in Section 2 is used to assess the minimum flexural residual strength that guarantees ductility. The second segment is subjected to its self-weight (Fig. 10a) and the total load transmitted by the upper segments (Fig. 10b). The self-weight of the segment is represented by means of a uniformly distributed load p = 16.2 kN/m and the force applied by the upper segments by $F = n_s \cdot P_s$, P_s being the self–weight of each individual segment (75.2 kN). The maximum bending moments are $M_{p,max}$ and $M_{F,max}$, depicted in Figure 10.

The cracking safety factor SF_{cr}, understood as a deterministic parameter, is defined as the ratio of the cracking bending moment of the cross – section (M_{cr}) and the total bending moment produced by the loads applied ($M_{tot} = M_{p,max} + M_{F,max}$). Figure 11a shows the curves that relate SF_{cr} and the eccentricity e for different numbers of segments in the pile. It is important to remark that the average flexural tensile strength of the concrete ($f_{ctm,fl}$) involved in the assessment of M_{cr} was calculated using the results of the bending tests shown in Fig.7 and imposing that $f_{ctm,fl} = f_{LOPm}$. Given the fact that the concrete age at the date of testing the segments was 4 days only and these had undergone vapour curing, the strength at 28 days was reduced by 15%.

The curves from Figure 11a confirm the results from the tests. They show that for an eccentricity of 0.25 m, the probability of cracking is low since SF_{cr} reaches values close to 1.5 for the maximum load (7 segments + key). On the contrary, for eccentricities close to 0.50 m, cracking occurs ($SF_{cr} < 1.0$) when the number of segments piled is higher than 5. Bearing in mind that e_e and e_i should

not be over 0.10 m in practice, the likelihood of cracking is small since for this eccentricity SF_{cr} is 3.2. In this context, only a minimum reinforcement should be placed in order to guarantee a ductile response in the unlike case of cracking.

Figure 11b shows the curves that relate $f_{R3m,min}$ and e for different values of n_s. Since the main goal is to compare these results with those obtained experimentally, the material and the load partial safety factors were fixed to 1.00 and average values for the material strengths were considered. The $f_{R3m,min}$ required to meet the ductility condition established in the MC 2010 may be calculated through Equation (4). Notice that a constant value of $f_{R3m,min}$ = 4,8 N/mm^2 is obtained regardless of n_s or e since M_{cr} is a mechanical property of the cross – section (dashed line in Fig. 11b).

On the other hand, for the alternative design philosophy proposed in this study, the mechanical requirement of the FRC was estimated considering characteristic values of loads and mechanical properties, which were then reduced by partial safety factors. Since the critical situation is observed in a transient stage, the partial safety factors for the loads are 1.35 for the self-weight and 1.00 for the load of the upper segments (the eccentricity should be considered as an accidental geometric imperfection), whereas the partial safety factor for the compressive and for residual tensile strengths of the FRC (γ_c) is 1.50. The M_d and the f_{cd} calculated in this way are included in Equation (5) to assess the minimum average value of f_{R3} for the alternative approach ($f_{R3m,alt}$), using ψ equal to 0.7 as proposed in the MC 2010 . Only the curve corresponding to a pile of 7 segments plus the key is showed (dotted line in Figure 11b).

Again, it is observed that the sectional response estimated with the numerical model agrees with the experimental results. At the moment of testing, the f_{R3m} of concrete of the segments was approximately 4.3 N/mm^2 (85% of f_{R3m} at 28 days for C_f = 60 kg/m^3, see Fig. 7). If $e_e = e_i$ = 0.5 m, this strength is exceeded when more than 5 segments are placed on the pile (required f_{R3m} equals 5.0 N/mm^2). The results also reveal that values of f_{R3m} higher than $f_{R3m,min}$ calculated according with the MC 2010 are obtained in case of having stacked more than five segments (n_s = 6 and $e \geq$ 0.48 m; n_s = 7 and $e \geq$ 0.40 m; n_s = 7 + key and $e \geq$ 0.36 m). For the other scenarios, although the f_{R3m} requirement might be less demanding, the $f_{R3m,min}$ would be used. For the eccentricity of 0.10 m considered in the project of Line 9 of Barcelona, the average residual strength calculated in service without any safety factor is 1.5 N/mm² (n_s = 7 + key and e = 0.10 m).

Notice that the ductility required by the MC 2010 would be fully activated only if a load approximately 3.2 times higher than the load expected during the transient stage (n_s = 7 + key and e = 0.10 m, Fig. 11a) is applied. In fact, this requirement ($f_{R3m,min}$ = 4,8 N/mm^2) provides a minimum residual strength that is high enough even to satisfy the ULS design of the segment. The reason for such result lays on the fact that these segments were designed not to crack. Consequently, the cracking load becomes the reference for the assessment of both SLS and ULS in terms of simple bending. As this load is also the basis for the assessment of the ductility requirement from the MC 2010, indirectly the minimum residual strength obtained complies with the ULS.

On the contrary, the alternative design philosophy proposed in this work yields a minimum residual strength of 3.2 N/mm² (Fig. 11b). Consequently, the ductility becomes active for a load 2.2 times higher than the load expected during the transient load stages, which is equivalent to an eccentricity e = 0.22 m if n_s = 7 + key (Fig. 11b). Such difference is attributed to the safety factors

introduced in the calculations. In this situation, the segment would be capable of showing ductility at a load level that is below the considered in the ULS and is more compatible with the requirements in the service stage, although a certain safety margin is maintained.

5 REPERCUSSION OF DUCTILITY CRITERIA

To evaluate the repercussion of the two approaches discussed in this study, the minimum average f_{R3m} estimated following each of them was translated into a required fibre content (C_f). For that, the values of $f_{R3m,min}$ calculated for a range of design eccentricities ranging from 0 to 0.15 m were divided by 0.85 to estimate the corresponding strength at 28 days. The latter was then used in Equation 7 to assess C_f. Figure 12 shows the curves that relate C_f and e for the critical situation of a pile composed by 7 segments plus the key.

As expected, the requirement from the MC 2010 leads to a constant C_f of 63.7 kg/m³ (65 kg/m^3 for production purposes). This value is difficult to justify from the technical, practical and economic point of view taking into account the specific circumstances of Line 9 of Barcelona. Consequently, the direct application of the requirement from the MC 2010 would render the use of fibres as the only reinforcement almost unviable for the example considered. In contrast, the new philosophy proposed here yields a C_f of 42.3 kg/m³ (45 kg/m^3). This represents a reduction of approximately 31% in the fibre consumption and provides enough ductility with a safety margin for the design load considered during stocking (all segments in the pile and accidental eccentricity e of 0.10 m).

6 CONCLUSIONS

The analysis performed in this study sheds light on a fundamental aspect related to the design of FRC tunnel segments that might have a direct practical repercussion. The following conclusions may be derived from the present work.

- The results from numerical simulations of the structural response of the segments under the storage conditions agree with the results obtained in the real-scale experimental program. The good agreement obtained indicates that the constitutive equation derived from the bending test of small-scale beams is representative of the behaviour of the FRC in the real segment subjected to the typical transient loads. This suggests that, in most situations, it might be enough to resort solely to numerical analysis based on small scale-test instead of performing a complex experimental programs with real-scale segments.

- In tunnels with segmental linings subjected mainly to compression in service and designed not to crack in the transient stages, the direct application of the ductility requirements from the MC 2010 may lead to a f_{R3} higher than the required value for the ULS. Such criterion may seem excessive taking into account that it responds to a transient stage and that the likelihood of cracking due to the applied loads is low (provided that $f_{ct,fl}$ is compatible with both the static and the dynamic loads expected and support configurations designed). If cracking occurs, the most probable scenario is that it will be the result of thermo-hygrometric induced stresses or a dynamic load very limited in time. In this context, the ductility required by the provisions

from the MC 2010 hardly ever will be activated considering the typical load observed in the transient stages.

- The alternative approach proposed in this study could be applied to estimate the required f_{R3} in tunnels that comply with 3 conditions: 1) the critical load occurring during the transient stages under controlled conditions; 2) the segments are designed not to crack and 3) are subjected to compression during service life. In this approach, the ductility is calculated considering the design values of both the mechanical parameters of the FRC and the loads by using the partial safety factors proposed in the MC 2010. The ductility obtained on this way will be more compatible with the load observed in the transient stages.

- For the application of the tunnel from the Line 9 of Barcelona, the $f_{R3m,min}$ estimated according with the MC 2010 is 4.8 N/mm². This mechanical requirement is related to a bending moment M_{cr}, which is 3.20 times higher than the bending moment expected during the transient stages. Consequently, the ductility provided by the fibres will only be fully activated at load levels far above the average observed in reality. On the contrary, in the alternative approach proposed in this study, a minimum average f_{R3} equal to 3.2 N/mm² is obtained. The letter is compatible with the loads expected during transient situations and the safety factors suggested in the MC 2010.

- Based on the results of the experimental program, the C_f estimated according with the MC 2010 and with the approach proposed here are 65 kg/m³ and 45 kg/m³, respectively. Even though ductility would be achieved in both of them for the load level expected in practice, the decrease in fibre consumption provided by the alternative approach could make the use of fibres viable without compromising the quality of the lining during the service life.

ACKNOWLEDGEMENTS

The authors want to thank the Ministry of Science and Innovation for the economic support received through the Research Project BIA2010-17478: Construction processes by means of fibre reinforced concretes. The first author would like to acknowledge the scholarship received from the China Scholarship Council.

REFERENCES

1. di Prisco M, Plizzari G, Vandewalle L., 2009. Fibre reinforced concrete: New design perspectives. Mater Struct 42(9), pp.: 1169-69.
2. Walraven J., 2009. High performance fibre reinforced concrete: progress in knowledge and design codes. Mater Struct 42(9), pp.: 1247-60.
3. Burguers R, Walraven J, Plizzari GA, Tiberti G., 2007. Structural behaviour of SFRC tunnel segments during TBM operations. In: World Tunnel Congress ITA-AITES, Prague (Czech Republic), 5-10 May 2007, pp.: 1461-1467.
4. Hilar M., Vítek P., 2012. Experimental loading tests of steel fibre reinforced and traditionally reinforced precast concrete segments for tunnel linings. Tunnel 21(4), pp.: 54-65.

5. de la Fuente A., Blanco A., Pujadas P., Aguado, A., 2011. Experiences in Barcelona with the use of fibres in segmental linings. Tunn. Undergr. Space Technol. 27(1), pp.: 60-71.

6. de la Fuente A., Blanco A., Pujadas P., Aguado A., 2012. Advances on the use of fibres in precast concrete segmental linings. Engineering and Concrete Future: Technology, Modelling & Construction. In: International Federation for Structural Concrete (fib). Fib Symposium, 22- 24 April 2012, Tel – Aviv (Israel). Text in Proceedings, pp.: 691-694.

7. DBV–Recommendation (German Concrete Association), 1992. Design principles of steel fibre reinforced concrete for tunnelling works, pp.: 19-29.

8. CNR DT 204/2006, 2006. Guidelines for the Design, Construction and Production Control of Fibre Reinforced Concrete Structures, Italian National Research Council - CNR.

9. CPH 2008. EHE-08: Spanish Structural Concrete Standard. Annex 14: Recommendations for the use of fibre reinforced concrete.

10. *fib* Bulletins 65-66 (2010), Model code 2010 Final Draft, 2010. fédération internationale du béton (*fib*), Lausanne (Switzerland).

11. Blanco A., Pujadas P., de la Fuente A., Aguado A., 2010. Comparative analysis of constitutive models of fibre reinforced concrete. Hormig. y Acer. 61(256), pp.: 83-101.

12. Blanco A, Pujadas P, de la Fuente A, Cavalaro S, Aguado A., 2013. Application of constitutive models in European codes to RC–FRC. Constr. Build. Mater. 40, pp.: 246–259.

13. Caratelli, A., Meda, A., Rinaldi, Z., 2012. Design according to MC2010 of fibre-reinforced concrete tunnel in Monte Lirio, Panama. Struct. Conc. 13(3), pp: 166-173.

14. de Waal, R.G.A., 1999. Steel fibre reinforced tunnel segments, ISBN 90-407-1965-9, Delft University of Technology (The Netherlands).

15. Kooiman, A.G., 2000. Modelling steel fibre reinforced concrete for structural design. Ph.D. thesis, Delft University of Technology (The Netherlands).

16. Blom C.B.M., 2002. Design philosophy of concrete linings in soft soils, ISBN 90-407-2366-4, Delft University of Technology (The Netherlands).

17. Cavalaro S.H.P., Blom C.B.M., Aguado A., Walraven J., 2011. New Design Method for the Production Tolerances of Concrete Tunnel Segments. J. Perform. Constr. Facil. 26(6), pp.: 824–34.

18. Haring, F.P., 2002. Stresses in assembly phase and serviceability phase in the lining of shield driven tunnels. Master thesis, Delft University of Technology (The Netherlands).

19. Sorelli L., Toutlemonde F., 2005. On the design of steel fibre reinforced concrete tunnel lining segments. In: 11th International Conference on Fracture, Turin (Italy), 20-25 March 2005, pp.: 6.

20. Groeneweg T.W., 2007. Shield driven in ultra-high strength concrete: reduction of the tunnel lining thickness. Master Thesis, Delft University of Technology (The Netherlands).

21. Burgers, R., Walraven, J.C., Plizzari, G.A., Tiberti G., 2007. Structural Behaviour of SFRC Tunnel Segments during TBM Operations. Underground Space the 4th Dimension of Metropolises: Proceedings of the World Tunnel Congress 2007 and 33rd ITA/AITES Annual

General Assembly, London (England), pp.: 1461–1467.

22. Tiberti G., Plizzari G., 2014. Structural behaviour of precast tunnel segments under TBM thrust actions. In: World Tunnelling Congress: Tunnels for a Better Life (WTC 2014), 9–15 May 2014, Foz do Iguaçu (Brazil). Text in CD of Proceedings.
23. Levi F., 1985. On minimum reinforcement in concrete structures. ASCE J. Struct. Eng. 111(12), pp.: 791–2796.
24. Chiaia B., Fantilli A.F., Vallini P., 2009. Combining fiber-reinforced concrete with traditional reinforcement in tunnel linings. Eng. Struct. 31(7), pp.: 1600-1606.
25. Chiaia B., Fantilli A.P., Vallini P., 2009. Evaluation of minimum reinforcement ratio in FRC members and application to tunnel linings. Mater. Struct. 42(3), pp.: 339-51.
26. Sugimoto M., 2006. Causes of shield segment damages during construction. In: International Symposium on Underground Excavation and Tunnelling. Bangkok, (Thailand).
27. Cavalaro S.H.P., Aguado A., 2012. Packer behaviour under simple and coupled stresses. Tunn. Undergr. Space Technol. 28, pp.: 159-173.
28. Cavalaro S.H.P., Blom C.B.M., Walraven J., Aguado A., 2012. Formation and accumulation of contact deficiencies in a tunnel segmented lining. Appl. Math. Mod. 36(9), pp.: 4422-4438.
29. Bakhshi M, Nasri V., 2014. Developments in design for fibre reinforced concrete tunnel segments. In: FRC 2014 Joint ACI-fib International Workshop. Fibre Reinforced Concrete Applications. 24-25 July 2014, Montreal (Canada), pp.: 441 - 452.
30. Bakhshi M., Nasri V., 2014. Review of international practice on critical aspects of segmental tunnel lining Design. In Proceedings of the 2014 North American Tunnelling (NAT) Conference. 22-25 June 2014, Los Angeles (USA), pp.: 274-282.
31. Bakhshi M., Nasri V., 2014. Guidelines and Methods on Segmental Tunnel Lining Analysis and Design – Review and Best Practice Recommendation. In Proceedings of the World Tunnel Congress 2014. May 9-15, 2014. Iguassu Falls (Brazil).
32. Bakhshi M., Nasri V., 2013. Structural design of segmental tunnel linings. In Proceedings of 3rd International Conference on Computational Methods in Tunnelling and Subsurface Engineering: EURO: TUN 2013. 17–19 April 2013, Ruhr University Bochum (Germany).
33. Camós C., Casas J.R., Molins C., 2014. An attempt to the determination of the partial safety factor for SFRC members subjected to bending forces. In: 8th RILEM International Syposium on Fibre Reinforced Concrete: challenges and opportunities, 19-21 September 2014, Guimaraes (Portugal) pp.: 1059-1069.
34. Gettu, R.; Aguado, A.; Ramos, G.; García, T., 2003. Viability analysis of the use of fibres as the unique concrete reinforcement for the precast segments of Barcelona's metro L9. Final Report, UPC BarcelonaTech (Spain), pp.: 49.
35. Gettu R., Barragán B., García T., Ramos G., Fernández C., Oliver R. 2004. Steel Fibre Reinforced Concrete for the Barcelona Metro Line 9 Tunnel Lining. In: 6th RILEM Symposium on FRC, 20-22 September, Varenna (Italy) 2004, pp.: 141-156.

36. Molins C., Arnau O., 2011. Experimental and analytical study of the structural response of segmental tunnel linings based on an in situ loading test: Part 1: test configuration and execution. Tunn. Undergr. Space Technol. 26 (6), pp.: 764-777.

37. Arnau O., Molins C., 2011. Experimental and analytical study of the structural response of segmental tunnel linings based on an in situ loading test. Part 2: Numerical simulation. Tunn. Undergr. Space Technol. 26 (6), pp.: 778-788.

38. Burguers, R., 2006. Non-linear FEM modelling of steel fibre reinforced concrete for the analysis of tunnel segments in the thrust jack phase. Final Report, University of Technology (The Netherlands), pp.: 115.

39. Pujadas P., Blanco A., Cavalaro, S.H.P., de la Fuente A., Aguado A., 2014. Fibre distribution in macro–plastic fibre reinforced concrete slab – panels. Constr. Build. Mater. 64, pp.: 496-503.

40. Pujadas P., Blanco A., Cavalaro S.H.P., de la Fuente A., Aguado A., 2014. Multidirectional double punch test to assess the post–cracking behaviour and fibre orientation of FRC. Constr. Build. Mater. 58, pp.: 214-224.

41. Blanco A., Pujadas P., de la Fuente A., Cavalaro S., Aguado A., 2015. Assessment of the fibre orientation factor in SFRC slabs. Composit. Part B 68(2), pp.: 343-354.

42. EN 14651, 2005. Test method for metallic fibered concrete. Measuring the flexural tensile strength (limit of proportionality (LOP), residual).

43. Barros J.A.O., Cunha V.M.C.F., Ribeiro A.F., Antunes J.A.B., 2005. Post-cracking behaviour of steel fibre reinforced concrete. Mater. Struct. 38(1), pp.: 47-56.

Table 1. Applications of precast FRC segments in tunnels (u.c.: under construction)

Name	Year	Country	Function	D_i (m)	h (m)	$\lambda = D_i/h$ ()	rebars
Metrosud	1982	IT	MT	5.8	0.30	19.3	No
Napoli Tunnel	1995	IT	MT	5.8	0.30	19.3	No
Heathrow Baggage Handling Tunnel	1995	UK	ST	4.5	0.15	30.0	No
2nd Heinenoord Tunnel	1999	NL	RT	7.6	0.27	28.1	No
Jubilee Line Extension	1999	GB	MT	4.5	0.15	30.0	No
Ecuador's Trasvases Manabi	2001	ECU	WTT	3.5	0.20	17.5	No
Hydraulic Tunnel Canal de Navarra	2003	ES	WTT	5.4	0.25/0.30	21.6/18.0	No
Oënzberg Tunnel	2003	SUI	RWT	10.8	0.30	36.0	No
Channel Tunnel Rail Link	2004	FR-UK	RWT	7.2	0.35	20.6	No
The Hofoldinger Stollen	2004	DE	WTT	2.9	0.18	16.1	No
San Vicente	2006	USA	WTT	3.2	0.18	17.8	No
Lötschberg	2007	SUI	RWT	4.5	0.20	22.5	No
Line 1 of the Valencia Metro	2007	VEN	MT	8.4	0.40	21.0	Yes
Beacon Hill Tunnels	2007	USA	RT	6.7	0.30	22.3	No
Gold Coast Desalination Plant	2008	AUS	WTT	2.8/3.4	0.20	14.0/17.0	No
Heathrow Express Ext. Tunnel to T5	2008	UK	RWT	5.7	0.22	25.9	No
São Paulo Metro Line 4	2009	BRA	MT	8.4	0.35	24.0	No
Heating Tunnel Amager - Copenhagen	2009	DEN	WTT	4.2	0.30	14.0	No
Fontsanta-Trinitat Tunnel	2010	ES	WTT	5.2	0.20	26.0	Yes
The Clem Jones Tunnel - Clem 7	2010	AUS	RT	11.3	0.40	28.3	No
Ems-Dollard Crossing	2010	DE-NL	GPT	3.0	0.25	12.0	No
Cuty West Cable Tunnel	2010	AUS	EP	2.5	0.20	12.5	No
Adelaide Desalination Plant	2010	AUS	WT	2.8	0.20	14.0	No
Extension of the FGC in Terrassa	2010	ES	RWT	6.0	0.30	20.0	Yes
Brightwater East	2011	USA	WTT	5.1	0.26	19.6	No
Brightwater Central	2011	USA	WTT	4.7	0.33	14.2	No
Brightwater West	2011	USA	WTT	3.7	0.26	14.2	No
East Side CSO Tunnel	2011	USA	WTT	6.7	0.36	18.6	No
Victorian Desalination Plant	2011	AUS	WTT	4.0	0.23	17.4	No
Monte Lirio Tunnel	2012	PAN	WTT	3.2	0.25	12.8	No
Lee Tunnel Sewer	u.c.	UK	WTT	7.2	0.35	20.6	No
Line 9 of Barcelona Metro	u.c.	ES	MT	10.9	0.35	31.1	Yes
Brenner Base Tunnel	u.c.	ITA-AUT	RT	5.6	0.20	28.0	Yes
The Wehrhahn Line	u.c.	DE	MT	8.3	0.45	18.4	No
Crossrail	u.c.	UK	RWT	6.2	0.30	20.7	No

Table 2. Composition of concrete

Material	Dosage (kg/m^3)
Cement type I 52.5R	400
Granitic sand 0-4 mm	846
Granitic aggregate 5-12 mm	443
Granitic aggregate 12-20 mm	550
Water	153
Superplastizicer	From 5.6 to 6.4
Fibres	20, 30, 40, 50 and 60

Figure 1. Temporary load stages of a segment: (a) demoulding; (b) stocking; (c) transport and (d) jack's thrust

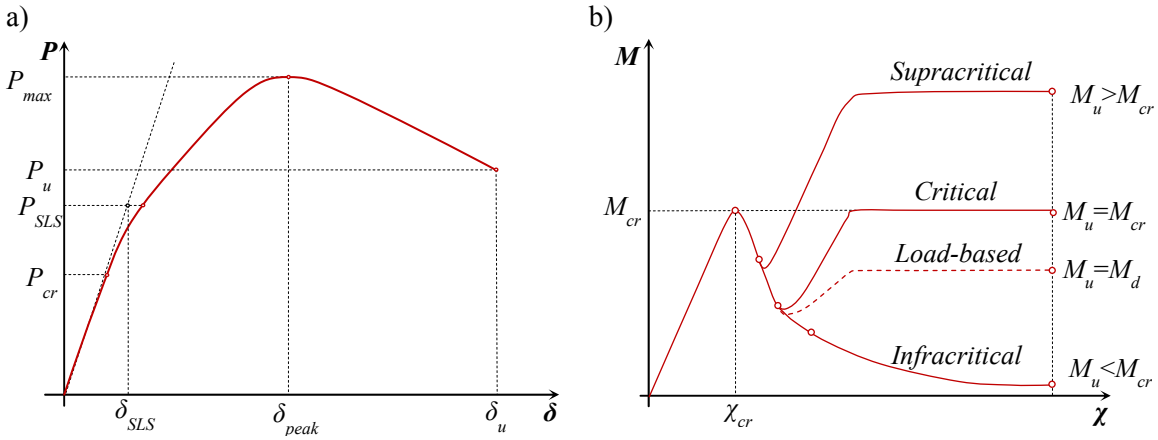

Figure 2. P-δ curve for a FRC structure (a) and M-χ diagram for different sectional responses (b)

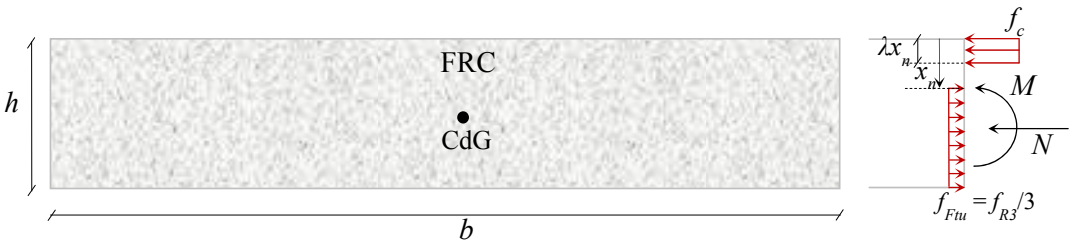

Figure 3. FRC cross – section of a precast segment subjected to axial stresses

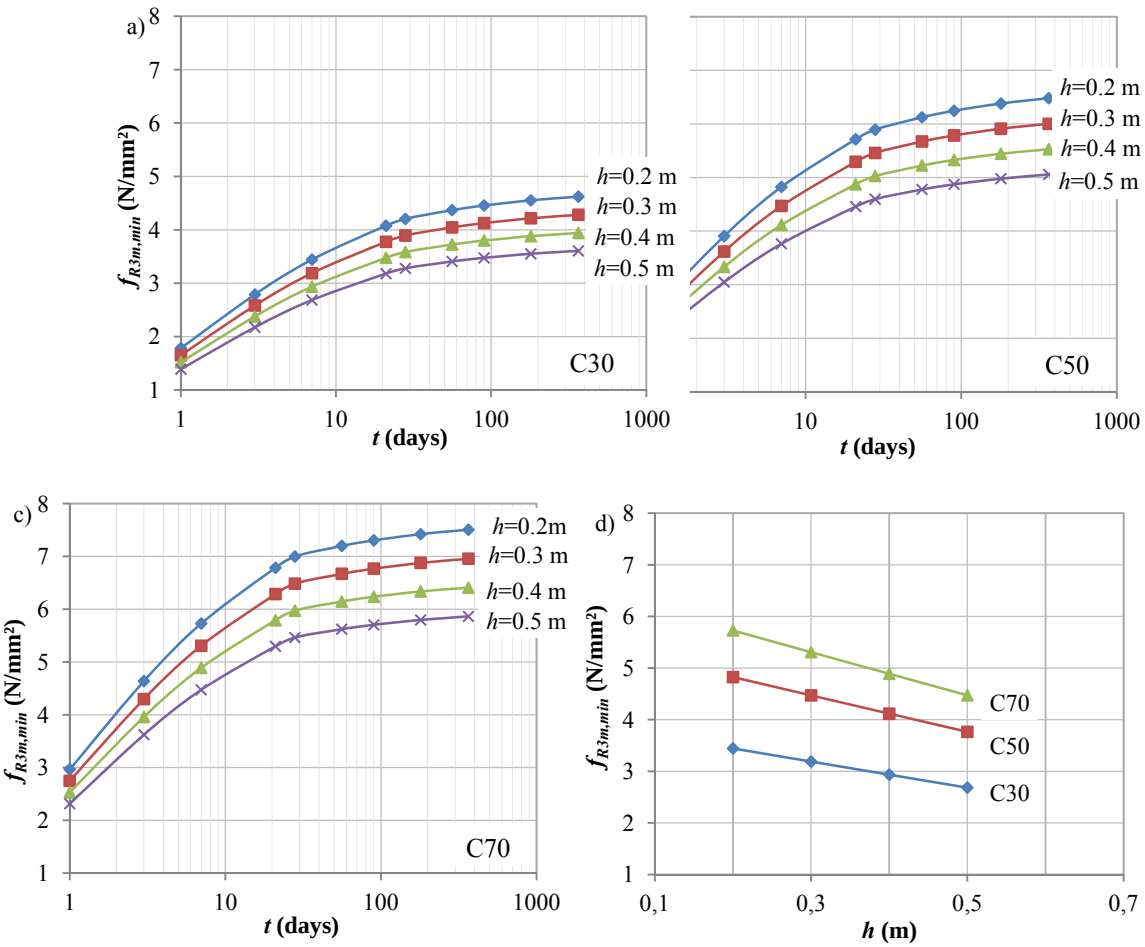

Figure 4. Age – dependency of the required $f_{R3m,min}$ for concrete classes (a) C30, (b) C50, (c) C70 and dependency of h on $f_{R3m,min}$ at 7 days (d)

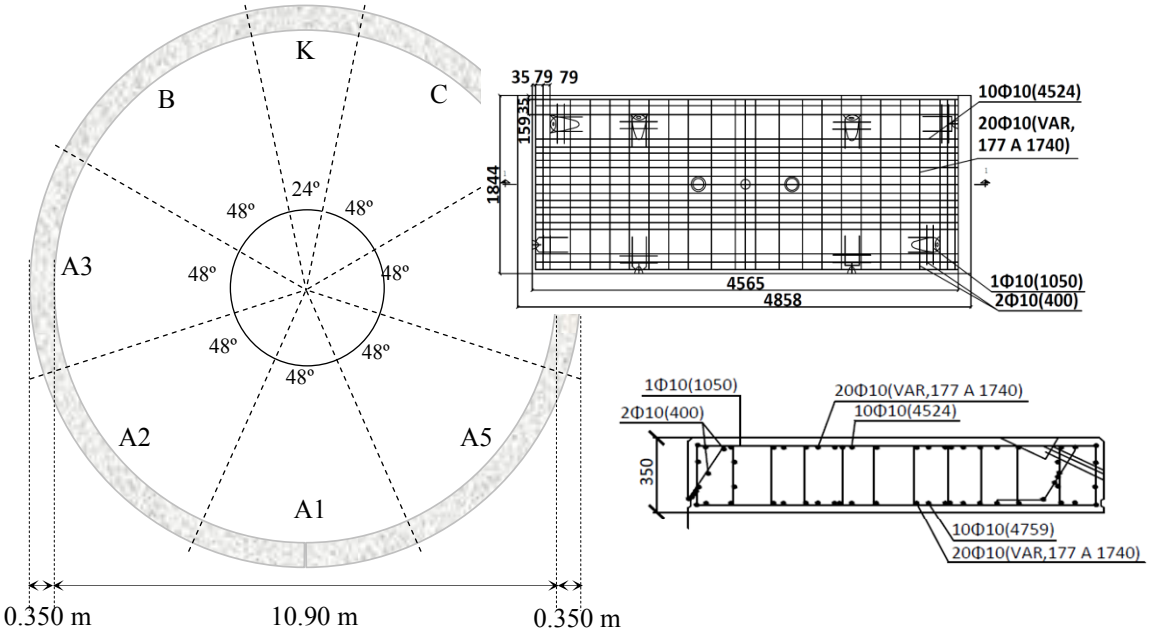

Figure 5. Ring dimensions of the Can Zam – Bon Pastor Stretch of Barcelona's Metro L9

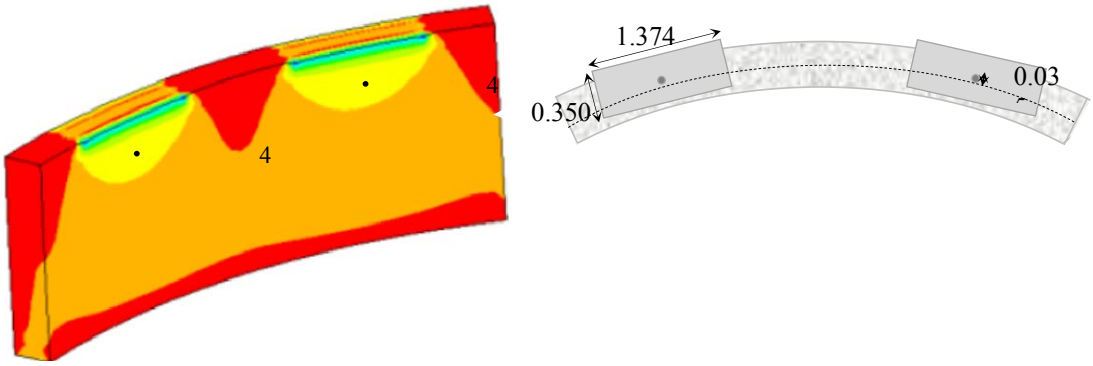

Figure 6. Dimensions of the jacks and eccentricity considered for the numerical analysis

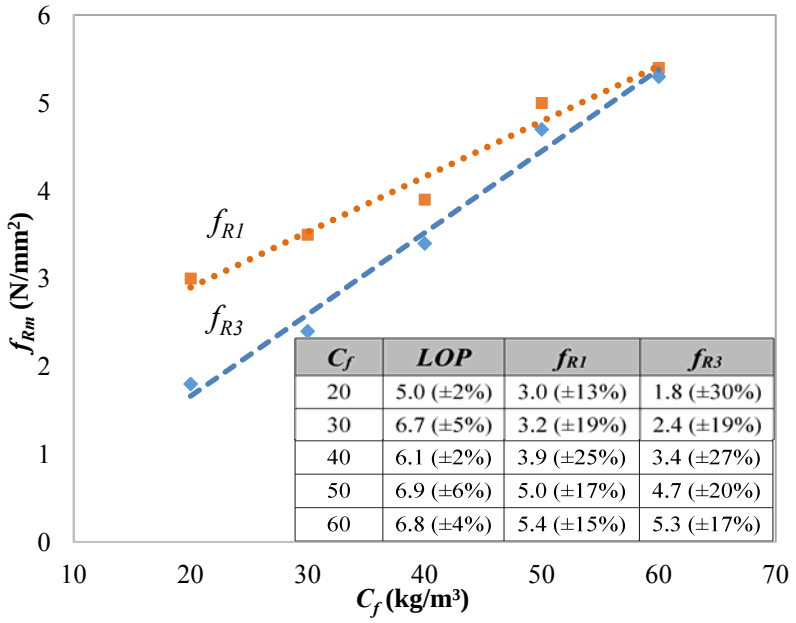

C_f	LOP	f_{R1}	f_{R3}
20	5.0 (±2%)	3.0 (±13%)	1.8 (±30%)
30	6.7 (±5%)	3.2 (±19%)	2.4 (±19%)
40	6.1 (±2%)	3.9 (±25%)	3.4 (±27%)
50	6.9 (±6%)	5.0 (±17%)	4.7 (±20%)
60	6.8 (±4%)	5.4 (±15%)	5.3 (±17%)

Figure 7. Average residual flexural tensile strength depending on fibre content

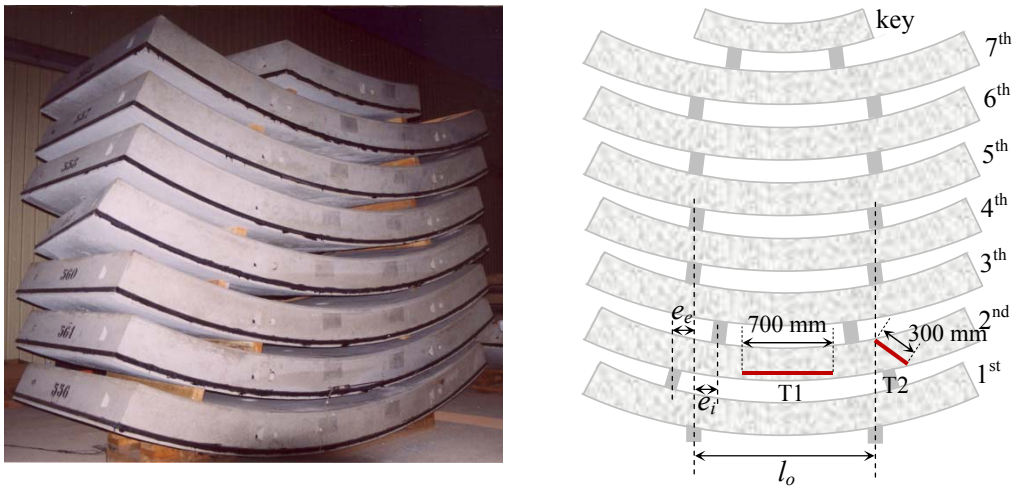

Figure 8. Test simulating the effects of the eccentricity in a pile of (a) 3 segments and (b) 7 segments plus a key

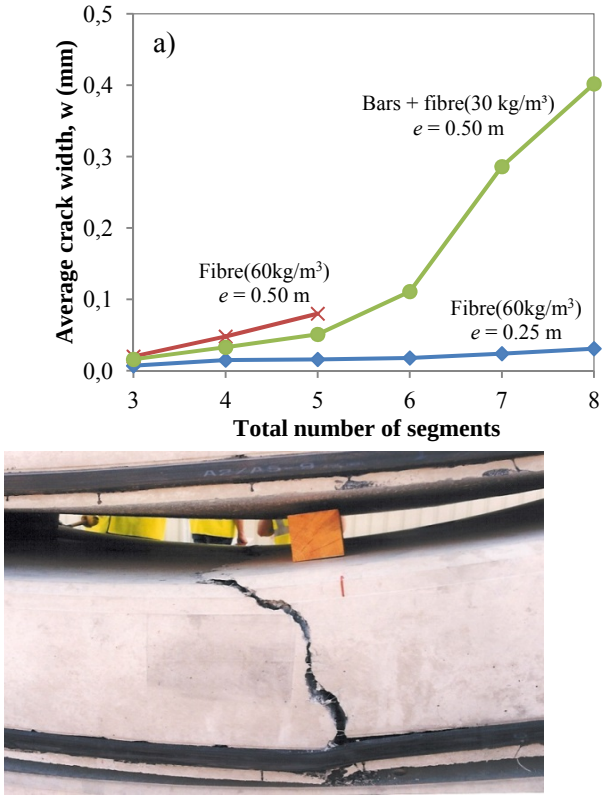

Figure 9. Detail of a) average crack width measured and b) expected brittle failure of segment reinforced only with 60 kg/m^3 of fibres and subjected to eccentricities of 0.50 m

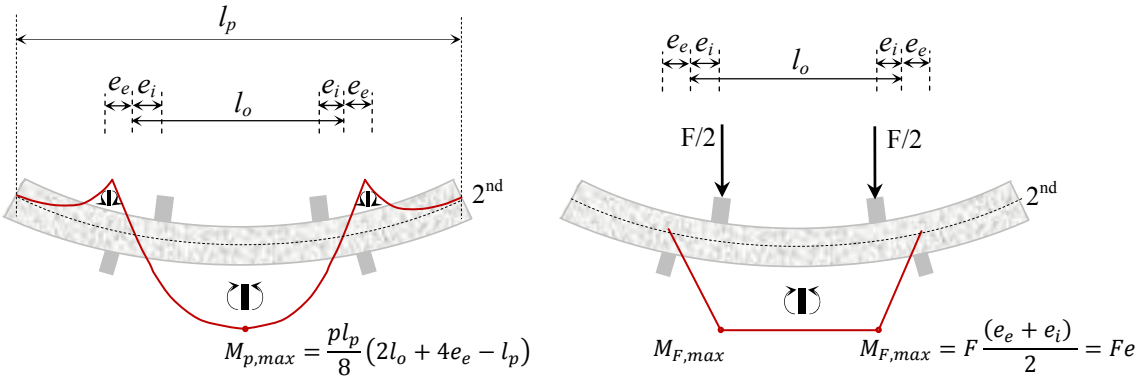

Figure 10. Bending moment diagrams for self-weight (a) and segments stocked (b)

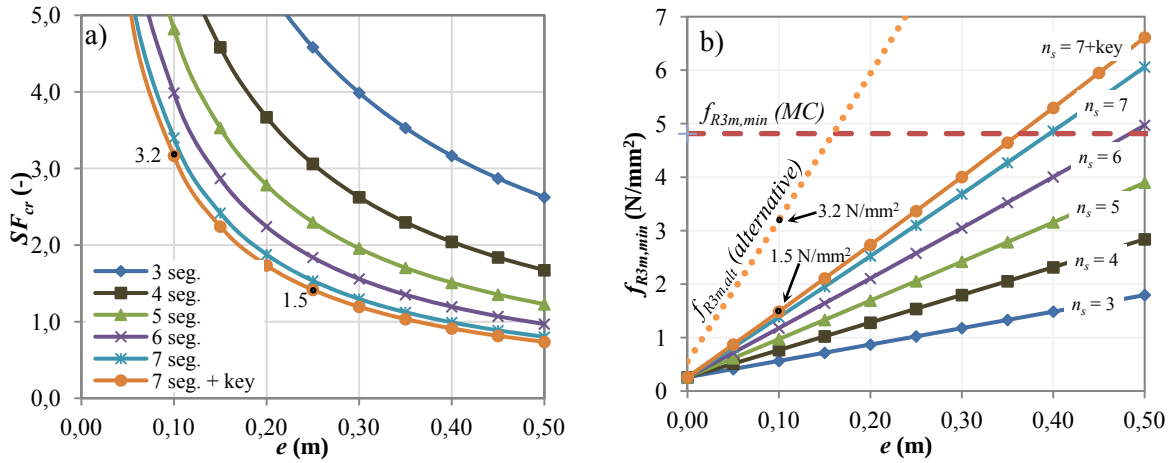

Figure 11. Variation of SF_{cr} (a) and $f_{R3m,min}$ (b) depending on eccentricity

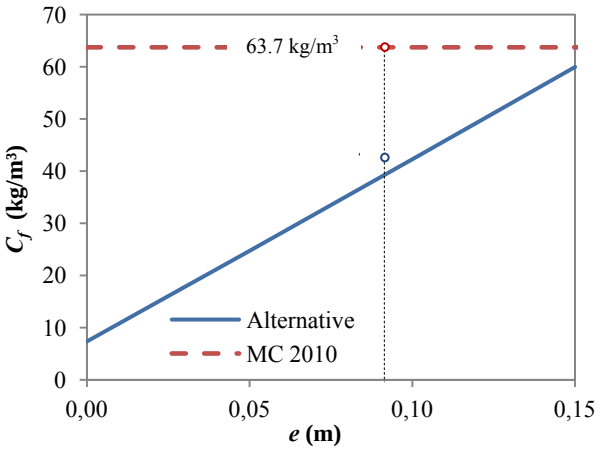

Figure 12. Curves C_f - e depending on the approach selected